Food Hydrocolloids 170 (2026) 111688

Contents lists available at ScienceDirect

Food Hydrocolloids

journal homepage: www.elsevier.com/locate/foodhyd

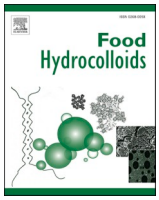

Physical properties and microstructure of hybrid processed cheeses formulated with plant protein and milk protein ingredients

Di Lu [a], Debashree Roy [a], Alejandra Acevedo-Fani [a], Harjinder Singh [a], Mark Waterland [b], Aiqian Ye [a,*]

[a] Riddet Institute, Massey University, Private Bag 11 222, Palmerston North, 4442, New Zealand
[b] School of Food Technology and Natural Sciences, Massey University, Private Bag 11 222, Palmerston North, 4442, New Zealand

ARTICLE INFO

Keywords:
Plant proteins
Hybrid cheese
Dairy analogues
Mung bean protein
Hemp proteins
Meltability

ABSTRACT

Hybrid processed cheese analogues (HPCAs) containing either mung bean (MPI) or hemp protein (HPI) with rennet casein (RC) at various ratios were prepared and analysed to understand their spatial and microstructural distribution and related physical properties, such as rheological properties, texture profile, meltability, and stretchability. In addition, protein composition and secondary protein structure were studied using SDS–PAGE and FTIR spectroscopy, while CLSM and TEM were employed to visualise the microstructure of the cheese matrix. Results indicated that plant protein types and concentration significantly affected the physical properties and microstructure of HPCAs. The addition of 30 % or more plant protein altered the physical and textural properties as well as the microstructure of the cheese analogues, with a decrease in β-sheet content and an increase in random coil structures. Mung bean protein–based HPCAs exhibit greater stretchability (e.g. 93.8 mm in 30 % MPI *vs* 41.53 mm in 30 % HPI), rheological, and textural properties, but not meltability (e.g. 1 % in 70 % MPI *vs* 48 % in 70 % HPI), compared with the hemp protein system at the same mixing ratios. This difference can be attributed to the size of the plant protein aggregation. All data were analysed by one-way ANOVA with Tukey's test ($p < 0.05$). These findings deepen our understanding of plant protein-based and hybrid cheeses, paving the way for optimised plant-based dairy alternatives.

1. Introduction

Processed cheese is a type of cheese manufactured by blending natural cheeses with emulsifying salts and other ingredients to enhance its melting properties, shelf life and flavour (McSweeney et al., 2017). They are extensively used in various culinary applications such as pizza, sauces and grilled cheese sandwiches (Dobson & Marangoni, 2023; Grasso et al., 2021). Recently, plant proteins have garnered considerable attention as consumers seek alternatives to dairy products. However, designing plant-based cheese products that match traditional milk-based cheeses presents substantial challenges (Grossmann & McClements, 2021), particularly in achieving the desired texture, meltability and flavour.

Processed plant-based cheese analogues in the market are made from non-dairy ingredients and primarily produced from polysaccharides (especially starches), vegetable oil (e.g. coconut, coca, and palm oils), minor fractions of plant protein (e.g. legume, nut, and seed proteins), salt (e.g. sodium citrate), texturiser (e.g. xanthan gum, agar, and alginic acid), and acidulant (e.g. acetic acid, citric acid, and lactic acid) (Grossmann & McClements, 2021; Kovačević et al., 2024). Commercially, numerous plant-based cheese formulations considerably rely on non-protein ingredients, such as starch and coconut oil, to provide structure and functionality to the final product, rather than protein, sacrificing the nutritional value (Grasso et al., 2021, 2022).

Blending plant proteins with dairy proteins offers a potential solution to maintain functional attributes and provide diverse nutritional values. In addition, interest in research on plant proteins and their functional contributions to hybrid cheeses and cheese analogues have significantly increased in recent years (Zhang et al., 2024). Soy and pea proteins are the most commonly used ingredients for developing plant-milk protein hybrid cheeses analogues (Farahmandfar et al., 2011; Mazinani et al., 2020; Omrani Khiabanian et al., 2020; Rinaldoni et al., 2014). Recently,

This article is part of a special issue entitled: 17th IHC published in Food Hydrocolloids.

* Corresponding author. Riddet Institute, Massey University, Private Bag 11 222, Palmerston North, 4442, New Zealand.
E-mail address: a.m.ye@massey.ac.nz (A. Ye).

https://doi.org/10.1016/j.foodhyd.2025.111688
Received 4 March 2025; Received in revised form 11 June 2025; Accepted 20 June 2025
Available online 21 June 2025

Table 1
Protein, fat, and moisture contents of processed hybrid cheese analogues.

	MPI100	MPI70	MPI50	MPI30	HPI100	HPI70	HPI50	HPI30	RC100
Protein (%, w/w)	18	18	18	18	18	18	18	18	18
Mung bean protein (%)	18	12.6	9	5.4	0	0	0	0	0
Hemp protein (%)	0	0	0	0	18	12.6	9	5.4	0
Rennet casein (%)	0	5.4	9	12.6	0	5.4	9	12.6	18
Fat (%, w/w)	20	20	20	20	20	20	20	20	20
Moisture (%)	42.8^{ad}	42.9^{ad}	42.2^{acd}	43.4^{a}	39.7^{b}	40.7^{bd}	40.7^{bd}	42.6^{ade}	40.3^{bce}

Values within a row not sharing a common superscript differ significantly ($p < 0.05$). The standard deviation of moisture values are less than 0.01. Ratios: MPI/HPI100 (100 % plant protein), MPI/HPI70 (70 % plant protein, 30 % rennet casein), MPI/HPI50 (50 % plant protein, 50 % rennet casein), MPI/HPI30 (30 % plant protein, 70 % rennet casein), RC100 (100 % rennet casein).

researchers have also explored the use of other plant proteins, such as faba, chickpea, lentil and mung bean proteins, as alternatives owing to their commercial availability and nutritional and functional properties (Garcia-Fontanals et al., 2023; Moradi et al., 2021; Rodrigues et al., 2021; Seleet et al., 2014; Tojan, 2021). For instance, Rodrigues et al. (2021) concluded that up to 25 % of milk proteins in cream cheese can be replaced with pulse proteins without significantly altering the overall composition and characteristics of the final product. A higher proportion of plant protein in hybrid cheese resulted in a weaker structure, poorer texture and a more open network than milk-based cheeses (Mazinani et al., 2020, 2021; Moradi et al., 2021). Although these studies highlight the effects of plant protein substitution on the final cheese properties, they do not provide insight into the underlying structural and physicochemical changes occurring within the cheese matrix at the microscopic level.

In this study, mung bean protein and hemp protein were selected to mix with rennet casein (RC) at various ratios to development hybrid processed cheese analogues (HPCAS), based on prior trial evaluating various plant proteins in processed cheese analogues (Lu et al., 2025). Results demonstrated differences in rheological, microstructural, and textural properties, with hemp protein showing higher scores (closer to rennet casein cheese, which scored 1) than mung bean protein. A separate pre-trial also confirmed differences in disulphide bond content and particle sizes between mung bean and hemp proteins (Supplementary Fig. S1 and Table S1), making it interesting to explore how these differences influence their interactions with caseins in the cheese matrix.

Mung beans contain about 25 %–28 % protein, and major proteins are globulins, which constitute 60 % of total protein (Li et al., 2023). The functional properties of mung bean protein are comparable to soybean protein, indicating similar surface hydrophobicity (Itoh et al., 2006; Mendoza et al., 2001; Tang & Sun, 2010; Yi-Shen et al., 2018). In addition, mung bean proteins are rich in vicilin-type proteins, which lack sulphur-containing amino acids. This affects their functional properties, such as gelation and protein network stability, by limiting disulphide bond formation (S. Shrestha et al., 2023). Hemp seeds contain around 25 % protein, comprising about 20 %–30 % albumin and 60 %–80 % globulins (edestin) (Chen et al., 2023; Xu et al., 2021). RC is commonly used in processed cheese (Noronha, Duggan, Ziegler, O'Riordan, & O'Sullivan, 2008; Noronha, Duggan, Ziegler, Stapleton, et al., 2008; Ye et al., 2009b; Ye & Hewitt, 2009a), which forms a continuous hydrated matrix, stabilising the oil-in-water interface by acting as an emulsifier. Emulsifying salts are added to the mixture to ensure adequate casein hydration and allow casein to emulsify the fat. Replacing RC with plant protein may change texture, rheological, and melting properties (Ørskov et al., 2021). A previous study explored replacing 30 % of milk with mung bean protein to develop cottage cheese (Tojan et al., 2024), finding that it reduced texture properties such as hardness and cohesiveness while increasing elasticity. However, it did not investigate the effects of varying substitution ratios on texture, microstructure and key functionality, particularly meltability and stretchability.

This study aimed to understand the spatial and microstructural distribution of mung bean and hemp proteins in hybrid cheese systems to gain insights into their interactions with RC and how microstructure affects cheese functionality. We hypothesize that the structure and functionality of these hybrid cheese systems differ due to the distinct properties and interactions of mung bean and hemp proteins with RC. To achieve this, we compared the protein composition and structure, rheological properties, microstructure, texture, meltability and stretchability between mung bean protein-based and hemp protein-based hybrid cheese systems. This will allow the optimisation of plant protein blends and have implications for modifying plant proteins to enhance their texture and physicochemical properties, tailoring them for specific applications in cheese products.

2. Materials and methods

2.1. Materials

Rennet casein (RC; SureProteinTM 779) containing 82 % protein was applied as milk protein and was obtained from Fonterra Co-operative Group Ltd., New Zealand. Mung bean protein isolate (85 %; MPI) were purchased from Bulk Powders New Zealand. Hemp protein isolate (70 %; HPI) and virgin coconut oil were purchased from Davis Trading Company, New Zealand. All chemicals used were of analytical grade and were obtained from Sigma Chemical Co., unless otherwise specified.

2.2. Preparation of HPCAs

HPCAs were made by mixing mung bean protein or hemp protein with RC at different mass ratios, namely, 100:0, 70:30, 50:50, 30:70, and 0:100, based on the total protein content. Each formulation was adjusted to a total sample mass of 30 g, with a final protein concentration of 18 % (w/w) on a wet basis. The formulation used was previously described by Ye et al.'s (2009b) study, with some modifications. Specifically, the formulation contained 18 % protein, 20 % coconut oil, 0.5 % sodium chloride, 0.5 % calcium sulphate, 0.1 % potassium sorbate, 2.8 % trisodium citrate, and water on a weight ratio basis. Subsequently, citric acid was added to control the pH of all samples around 5.4. To achieve an 18 % protein concentration, the protein powder amount was adjusted to accommodate variations in protein content among different sources. HPCAs were prepared using a Rapid Visco Analyser (RVA-4; Newport Scientific Pty Ltd, Warriewood, NSW, Australia). HPCAs samples of 30 g were prepared in an aluminium cell fit with a polycarbonate paddle (Lu et al., 2025). All dry ingredients and oil were manually blended with water for 5 min and then hydrated for 1 h at room temperature in an aluminium cell. The mixture was loaded onto the RVA instrument and processed as follows: equilibration at 50 °C, followed by heating to 90 over 4 min, maintaining at 90 °C for 10 min. The sample was then cooled to 50 °C at a rate of 0.2 °C/s, mixing at 300 rpm from heating to cooling stages. The HPCAs developed were named as HPI100, HPI70, HPI50, HPI30, MPI100, MPI70, MPI50, MPI30, and RC100. For example, HPI100 contains only hemp protein, while HPI70 contains 70 % hemp protein and 30 % RC, and so on. All samples with protein, fat, and moisture ratios are shown in Table 1. All samples were prepared in

different sizes for various types of analysis and stored at 4 °C for further use.

2.3. Sodium dodecyl sulphate–polyacrylamide gel electrophoresis (SDS–PAGE)

SDS–PAGE was used to characterise the protein profiles of the HPCAs, under reducing and non-reducing conditions. HPCAs include samples containing plant protein and rennet casein in the following ratios: 100:0, 90:10, 80:20, 70:30, 50:50, 30:70, 20:80, 10:90, and 0:100. Each cheese sample was prepared in a sample buffer (5.55 mg/mL) containing 0.5 M Tris-HCl, pH 6.8, 2 % (w/v) SDS, 150 mL/L glycerol, 0.0025 % (w/v) bromophenol blue, and 5 % (v/v) 2-mercaptoethanol only in the case of reducing conditions. Subsequently, the sample was boiled for 10 min and cooled at room temperature. Each well of the gel with a 16 % resolving gel and 4 % stacking gel was loaded with 5 μL of the sample containing 0.1 % (w/w) of proteins or molecular weight markers (Catalog # 161–0377, Bio-Rad, USA). A PowerPac Basic (Bio-Rad, USA) was used to conduct electrophoresis at a constant voltage of 150 V in a tris-glycine running buffer (0.025 M Tris, 0.192 M glycine and0.1 % (w/v) SDS). After electrophoresis, the gels were stained with Coomassie Brilliant Blue R-250 staining solution (Bio-Rad, USA) for 3 h, followed by destaining with a 10 % isopropanol/glacial acetic acid solution overnight using a shaker (OM6, RATEK, Australia) (Beghdadi et al., 2022; Hu et al., 2023).

2.4. Dynamic rheological analysis

Rheological properties were measured using a stress-controlled rheometer (Physica MCR 302, Anton Paar, Austria) equipped with a 20 mm diameter parallel plate with a 2.0 mm gap. HPCAs were removed from the aluminium cell and then rolled into a slice (cheese slice) with a uniform thickness of approximately 2.2 mm. Cheese slices were carefully cut into 20 mm diameter discs using a cylindrical cutter and equilibrated at room temperature in a plastic bag for 1 h before the experiment. The cheese discs were placed on the surface of the lower plate. The upper serrated plate (parallel plate) was lowered until it reached a 2 mm gap distance, and the sample was trimmed and left to rest for 15 min in the rheometer. Meanwhile, the exposed edge of the samples was coated with a thin layer of mineral oil to minimize moisture loss during the measurement. The linear viscoelastic range was obtained by conducting an amplitude sweep at 1 Hz as the percentage of strain values varied from 0.01 % to 100 %. Subsequently, the linear region was selected (0.5 % of strain amplitude), and a frequency sweep was conducted at 20 °C with the frequency varying from 0.01 to 10 Hz. This was followed by a temperature sweep at a constant frequency of 1 Hz and a constant strain amplitude of 0.5 %. In addition, the temperature was increased from 20 °C to 90 °C at 3 °C/min using a Peltier heating element. Moreover, the storage modulus (G'), loss modulus (G''), and loss tangent (tan δ) were determined.

2.5. Microstructure

Confocal laser scanning microscopy (CLSM) and transmission electron microscopy (TEM) analyses were conducted at the Manawatu Microscopy and Imaging Centre (Massey University, Palmerston North, New Zealand).

2.5.1. CLSM

Microstructural analysis of HPCAs prepared using RVA was conducted using a Confocal Laser Scanning Microscope (ZEISS LSM 900, Germany). Fresh cheese samples prepared using RVA were cut into thin layers and stained with a fluorescent dye solution containing 1 % Nile Red (1 mg/ml in acetone), which stains the fat phase, and 1 % Fast Green FCF (1 mg/ml in Milli-Q water), which stains the protein phase, for 10 min before imaging. Fast Green FCF and Nile Red were excited with He–Ne laser at 633 nm and argon laser at 488 nm, respectively (Auty et al., 2001; Gallier et al., 2012). Representative images are reported, which were captured using a 20 × objective lens.

2.5.2. TEM

HPCAs were examined using TEM. The samples were first sliced into small cubes (1 mm × 1 mm × 1 mm) and embedded in 3 % agarose. According to Li et al. (2021), the samples were placed in 3 % glutaraldehyde in 0.1 M sodium cacodylate (pH 7.2) for at least 24 h. Subsequently, the samples were washed in buffer and dehydrated using a graded acetone series. Finally, the samples were embedded in moulds with fresh resin and cured in a 60 °C oven for 48 h. Light microscope sections (1 mm) were cut using a glass knife on an ultramicrotome (Leica EM UC7, Germany) and heat-fixed onto glass slides. These sections were stained with 0.05 % toluidine blue and viewed under a light microscope. Thin sections (around 100 nm) were cut using a diamond knife, stretched with chloroform, and mounted on grids using a Coat-Quick 'G' pen (Daido Sangyo, Japan). Afterward, the grids were stained and washed and then stained with lead citrate, followed by another wash using Milli-Q water. The samples were imaged with a Tecnai G2 Spirit BioTWIN (FEI Company, Czech Republic) paired with a Veleta TEM camera (Olympus SIS, Germany).

2.6. Texture profile analysis (TPA)

TPA was conducted using TAXT.plus (Stable Micro Systems Ltd., Godalming, Surrey, UK). Cheese samples prepared using the RVA (section 2.2) were transferred to moulds and stored at 4 °C. Afterward, the cheese samples were cut into cylinders with a height of 20 mm and a diameter of 15 mm for the analysis. A 50 mm compression cylinder probe (P/50) attached to a 50 kg load cell was utilised for all TPA measurements. Two compression-decompression cycles were conducted with a pre-test speed of 1.00 mm/s, test speed of 5.00 mm/s, and post-test speed of 5.00 mm/s to compress the cheese sample to 75 % of its initial height. TPA parameters were measured as hardness, springiness, cohesiveness, chewiness, and resilience. The standard deviation of the results was calculated.

2.7. Meltability and stretchability

The meltability of HPCAs prepared with RVA was measured using a modified Schreiber melt test (Kosikowski, 1977). Cheese samples were rolled into slices with a uniform thickness of approximately 5 mm and 30 mm in diameter, placed on glass Petri dishes, and heated in an oven at 170 °C for 10 min. Radius of expansion in four directions (0°, 90°, 180°, and 270°) was measured after cooling to 20 °C. The melt index was the average value of the four radius readings.

A stretchability test was conducted using a TA-HD plus Texture analyser (Stable Micro Systems Ltd., Godalming, Surrey, UK) with a modified cheese stretchability rig, which included an in-house built post hook and a base pot (Supplementary Fig. S2). HPCAs were prepared using the formulation discussed in section 2.2 but heated in a water bath at 90 °C for 10 min at 300 rpm, allowing for the production of a large sample size. The samples (150 g) were weighed and evenly distributed in the pot. Subsequently, the base pot and post hook with the cheese sample were heated in the oven at 95 °C for 15 min. To minimize drying during heating, the cheese was covered with aluminium foil. Moreover, the hook–sample–pot assembly was placed on TA, and a thermometer (temperature probe) was inserted into the cheese. Once the temperature reached 60 °C, the test was initiated by pulling the hook out of the melted sample. The test speed and distance were set to 10 mm/s and 200 mm, respectively.

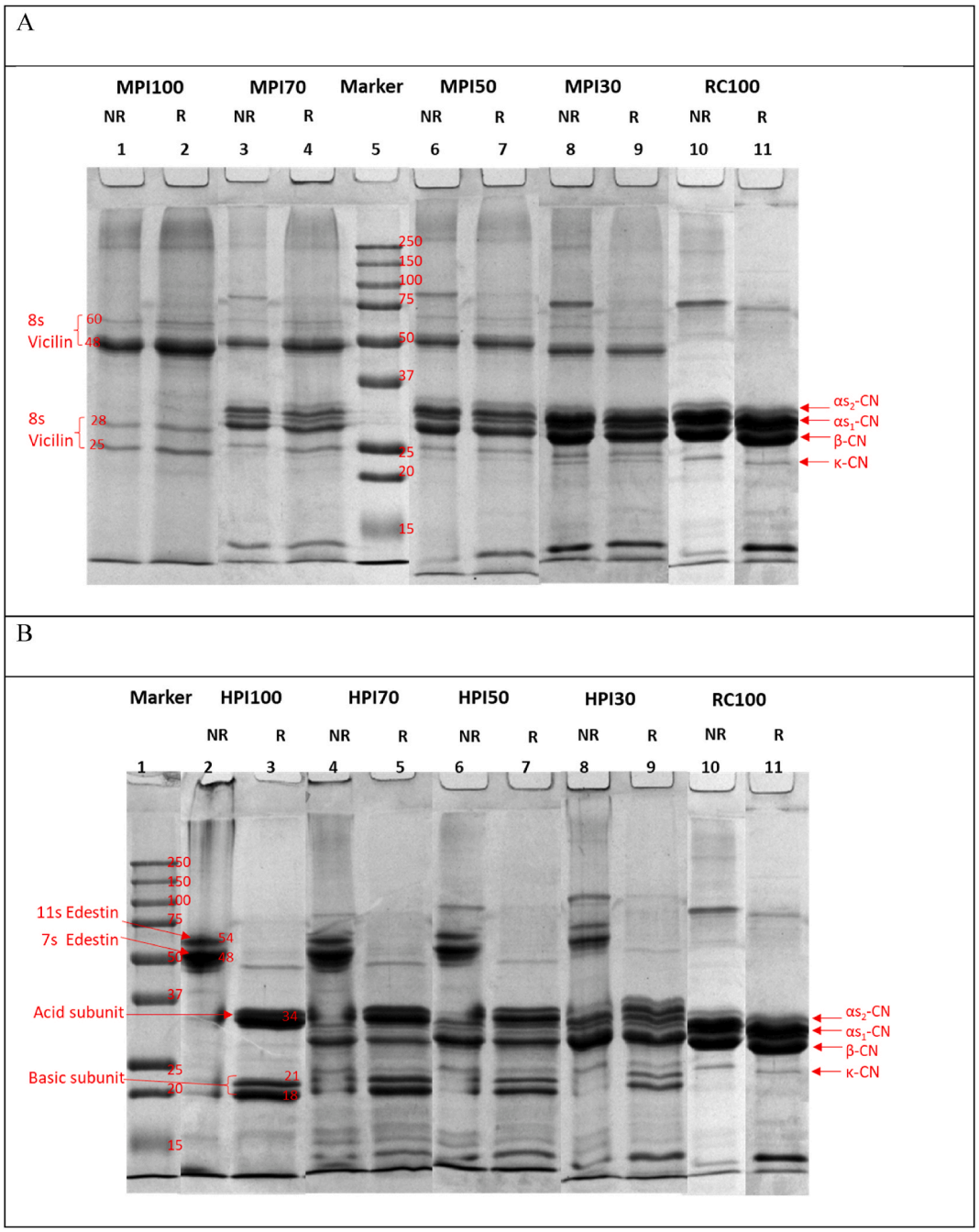

Fig. 1. SDS-PAGE profile of hybrid processed cheese analogues (HPCAs) made with mung bean protein (MPI) (A) or hemp protein (HPI) (B) and rennet casein (RC) at varying ratios. Ratios: MPI/HPI100 (100 % plant protein), MPI/HPI70 (70 % plant protein, 30 % rennet casein), MPI/HPI50 (50 % plant protein, 50 % rennet casein), MPI/HPI30 (30 % plant protein, 70 % rennet casein), RC100 (100 % rennet casein). The samples were prepared under reducing (R) and non-reducing (NR) conditions. Molecular weight marker in kDa; α_{s1}-CN: α_{s1}-casein; α_{s2}-CN: α_{s2}-casein; β-CN: β-Casein; κ-CN: κ-Casein.

2.8. Analysing protein structure with Fourier transform infrared (FTIR) spectroscopy

Protein structure changes in HPCAs with different plant protein to rennet casein ratios were evaluated via FTIR spectroscopy(Gawat et al., 2024; Salgado et al., 2023). Cheese samples were cut into thin layers before being placed directly on the crystal and pressed down onto it. The analysis was conducted using a Nicolet™ iS™ 5 FTIR Spectrometer (Thermo Fisher Scientific Inc., Waltham, MA, USA) with an iD7 ATR accessory (Thermo Fisher Scientific Inc., Waltham, MA, USA). The scan was conducted between 4000 and 450 cm−1 with a resolution of 2 cm^{-1}. The background spectrum was initially obtained and automatically subtracted from every acquisition and was reset after scanning for 1 h. For each sample spectrum, 32 scans were accumulated and averaged.

The deconvolution of the amide I region (1600 and 1700 cm^{-1}) was done for further quantitative analysis. First, each spectrum was processed for baseline correction and smoothed using a 25-point Savitzky-Golay filter with a second-order polynomial to improve the signal-to-noise ratio in Origin® software (2021b). Next, automatic peak fitting was conducted using the second derivative, and subsequent peak fitting was done using the Gaussian assumption implemented in the Peakfit 4.12 software (Systat Software, Inc., CA, USA). The resulting peaks after deconvolution were identified based on known IR spectral data for

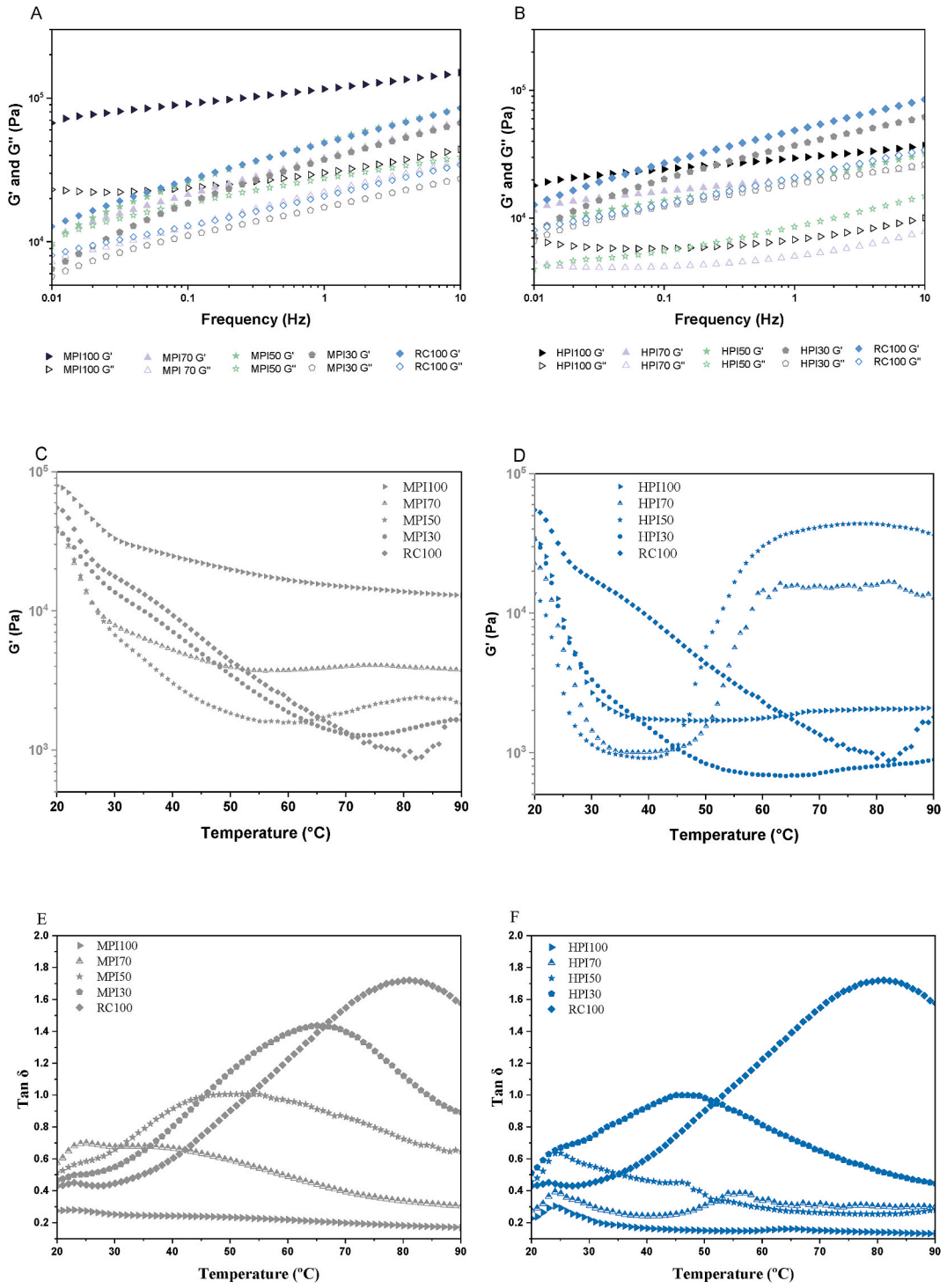

Fig. 2. Rheological properties of hybrid cheese analogues made with mung bean protein (MPI) or hemp protein (HPI) and rennet casein at varying ratios. Storage modulus (G′) and loss modulus (G″) *vs.* frequency at 20 °C, γ = 0.5 % (A, B). G' (C, D) and tan δ (E, F) *vs.* temperature (ω = 1 Hz, γ = 0.5 %). Ratios: MPI/HPI100 (100 % plant protein), MPI/HPI70 (70 % plant protein, 30 % rennet casein), MPI/HPI50 (50 % plant protein, 50 % rennet casein), MPI/HPI30 (30 % plant protein, 70 % rennet casein), RC100 (100 % rennet casein).

protein secondary structures. Several iterations were conducted until the fit converged with a final fitting curve that achieved a corrected $R^2 \geq 0.99$. Finally, the area under each peak was evaluated against the total area and expressed as a percentage. Reported values for β-sheet and β-turns are accumulated values of more than one peak.

2.9. Statistical analysis

All experiments were performed in triplicate (unless otherwise specified). Results are reported as mean values and standard deviations. To identify differences between HPCAs formulations, the data were subjected to one-way ANOVA analysis using SPSS, followed by Tukey's comparison difference. Differences were considered significant at a level of $p < 0.05$.

3. Results and discussion

3.1. Protein composition

The major protein constituents of HPCAs were identified using SDS–PAGE. The mung bean protein-based cheese sample (MPI100) exhibited SDS–PAGE bands with molecular weights ranging from 80 to 26 kDa, with no major distinctions between PAGEs under reducing and non-reducing conditions (Fig. 1A). Bands at ~60, 48, 28 and 25 kDa, corresponding to sub-units of vicilin-like globulin, remained unchanged under reducing conditions (lane 1 & 2, Fig. 1A). This is consistent with reports indicating that 8S vicilin, which lacks disulphide bonds, contains 89 % protein and no sulphur-containing amino acids (Shrestha et al., 2023; Yi-Shen et al., 2018). However, this study did not observe the 7S (~16 and ~28 kDa) and 11S (~24 and ~40 kDa) subunits, likely owing to differences in mung bean protein variety and isolation methods compared to previous reports. For casein cheese (RC100, lane 10 & 11), α_{s1}-and β-caseins were observed as the two most predominant protein bands in both non-reducing and reducing conditions, while α_{s1}-and κ-caseins presented as two faint bands. For cheese samples made by blending MPI and RC, all proteins from both MPI and RC were observed in both the PAGEs under reducing and non-reducing conditions, indicating no complexation between the caseins and mung bean protein. This is consistent with the study results of Beghdadi et al. (2022), who found that co-heating casein with pea proteins (7.5:2.5) did not result in interaction between the two, because no new complexes were observed in SDS–PAGE. Instead, the pea protein formed its own gel at a low pH, acting as a 'space-filling gel' within the casein gel.

Hemp protein comprises ~20 %–30 % albumin and 60 %–80 % edestin (globulin) (Chen et al., 2023; Xu et al., 2021). Edestin is further divided into 7s and 11s protein fractions (Fig. 1B). In non-reducing SDS–PAGE, a band around 54 kDa was attributed to the edestin monomer, which disappeared under reducing conditions owing to the cleavage of disulphide bonds, resulting in three distinct bands at ~34, ~21, and ~18 kDa for the acidic and the basic sub-units (Do et al., 2024). Meanwhile, a band around 48 kDa was associated with the 7s globulin sub-unit, with little effects under reducing conditions. In cheese samples made by mixing HPI with RC, for instance, under non-reducing conditions, a thick band at 54 kDa was observed in HPI50 (lane 6, Fig. 1B), and both β-casein and α_{s1}-casein were also observed. However, the band intensities of α_{s1}-casein and α_{s2}-casein were weaker than that in reducing PAGE. The observed decrease in α_{s1}-casein and α_{s2}-casein band intensities in non-reducing conditions may indicate potential interactions between α_{s2}-casein and HPI proteins. In addition, the reduction of the α_{s1}-casein and α_{s2}-casein band intensities was not observed in case of MPI-based hybrid cheese samples under non-reducing conditions (Fig. 1A) further suggested the potential interactions between α_{s2}-casein and HPI proteins. Given that α_{s2}-casein contains two disulphide bonds, it is hypothesized that disulphide linkages could form between α_{s2}-casein and HPI. However, under reducing conditions, the α_{s2}-casein band became less distinguishable, likely due to overlap with the acidic sub-unit of HPI. Preliminary results suggest a potential interaction between α_{s1}-casein, α_{s2}-casein, and HPI, the exact nature of these interactions via disulphide bond exchange or non-covalent association requires further investigation.

3.2. Rheological properties of HPCAs

3.2.1. Frequency sweep

A frequency sweep test was performed on HPCAs over a range of angular frequencies (0.01–10 Hz) within the linear viscoelastic region (0.5 % strain level). Parameters of interest are the storage modulus (G′) and loss modulus (G″), which respectively characterise the elastic (solid-like) and viscous (liquid-like) components of cheese response to deformation. Fig. 2A and B demonstrate that all cheese samples exhibited more elastic-like behaviour, as G′ was higher than G″ throughout the tested frequency range.

In the mung bean protein-based HPCAs (Fig. 2A), MPI exhibited the highest G′ values and was relatively independent of frequency changes, indicating superior elastic properties and a more rigid structure. In addition, the lower frequency dependence suggests that non-covalent bonds, such as hydrophobic interactions and hydrogen bonds, might control the gel network (Zhu et al., 2021). By contrast, RC100 cheese had lower G′ and G″ values and tended to be more frequency-dependent, indicating a more dynamic protein network. Mixing mung bean protein with casein at different ratios resulted in a weaker gel with a less integrated network, as observed by the lower G′ values at 0.01 Hz compared with MPI100 and RC100. With increasing frequency, the G′ and G″ values of MPI70, MPI50, and MPI30 increased, likely owing to the re-organisation of protein networks under stress. Similar observations were found in hemp protein-based hybrid cheese samples (Fig. 2B). HPI100 cheese was less frequency-dependent than RC100 cheese, and mixtures of hemp protein and RC exhibited weaker networks, likely owing to the incomplete integration of the two proteins. In addition, HPI100 cheese was less stiff than MPI100 owing to significantly lower G′ values. The G′ and G″ values of HPI70 were more similar to HPI100 than RC100, indicating that hemp protein more strongly influences the structure of the hybrid cheese at a 70 % concentration, whereas MPI70 showed a similar trend to RC100. This observation indicates that hemp protein is more disruptive to the casein-casein interactions than mung bean protein.

Rheological results of the present study are consistent with those of several previous studies on the effects of plant proteins on rheological properties of plant protein hybrid cheeses or plant protein–casein mixtures (Beghdadi et al., 2022; Beliciu & Moraru, 2011; Li et al., 2018; Silva et al., 2019a; Zhang et al., 2024). These studies concluded that casein and plant proteins did not co-aggregate in the mixtures during heating, and that each type of protein formed its own independent network with G′ and G″ decrease, indicating a weaker structure in mixed system.

3.2.2. Temperature sweep

When cheese is heated, there is a dramatic decrease in the total number and strength of bonds in the cheese matrix owing to the shrinkage of the para-casein network (Fox et al., 2017a). This is indicated by the decrease in G′ and G″ (Fig. 2C and D) and the increase in tan δ (G″/G′) (Fig. 2E and F). Cheese samples with a tan $\delta < 1$ exhibit solid behaviour, while those with a tan $\delta > 1$ exhibit more liquid-like behaviour. The transition of cheese from solid to liquid (tan $\delta = 1$) occurs at a specific temperature, known as the transition temperature. In the initial heating segment, all samples exhibit an increase in tan δ to ~25 °C, which is consistent with the melting of coconut oil (Dobson & Marangoni, 2023) (Fig. 2E and F). Neither mung bean nor hemp protein-based cheeses (MPI100, MPI70, HPI100, HPI70 and HPI50) exhibited significant softening as the temperature increased to 90 °C, maintaining tan δ values at <1 (G′ > G″). This indicates that plant protein did not exhibit softening and viscous behaviour with increasing temperature. Moreover, the addition of plant protein to cheese reduced tan δ, suggesting that plant proteins disrupted casein-casein interactions. The transition temperature and tan δ values increased with increasing levels of RC. For instance, MPI50 and MPI30 had transition temperatures at 45 °C, and RC100 transitioned at 55 °C. In addition, tan δ values peaked at 50 °C, 65 °C and 82 °C with values of 1, 1.4 and 1.7, respectively, indicating enhanced formation of the casein-casein network, which corresponds with other findings in the literature for commercially processed cheese (Dobson & Marangoni, 2023; Noronha, Duggan, Ziegler, O'Riordan, & O'Sullivan, 2008). After reaching the peak temperature, tan δ decreased, likely owing to increased hydrophobic-induced protein interactions (Bryant & McClements, 1998).

When the same amount of hemp or mung bean protein was mixed with casein protein (i.e., MPI50 *vs.* HPI50, MPI30 *vs.* HPI30), the tan δ

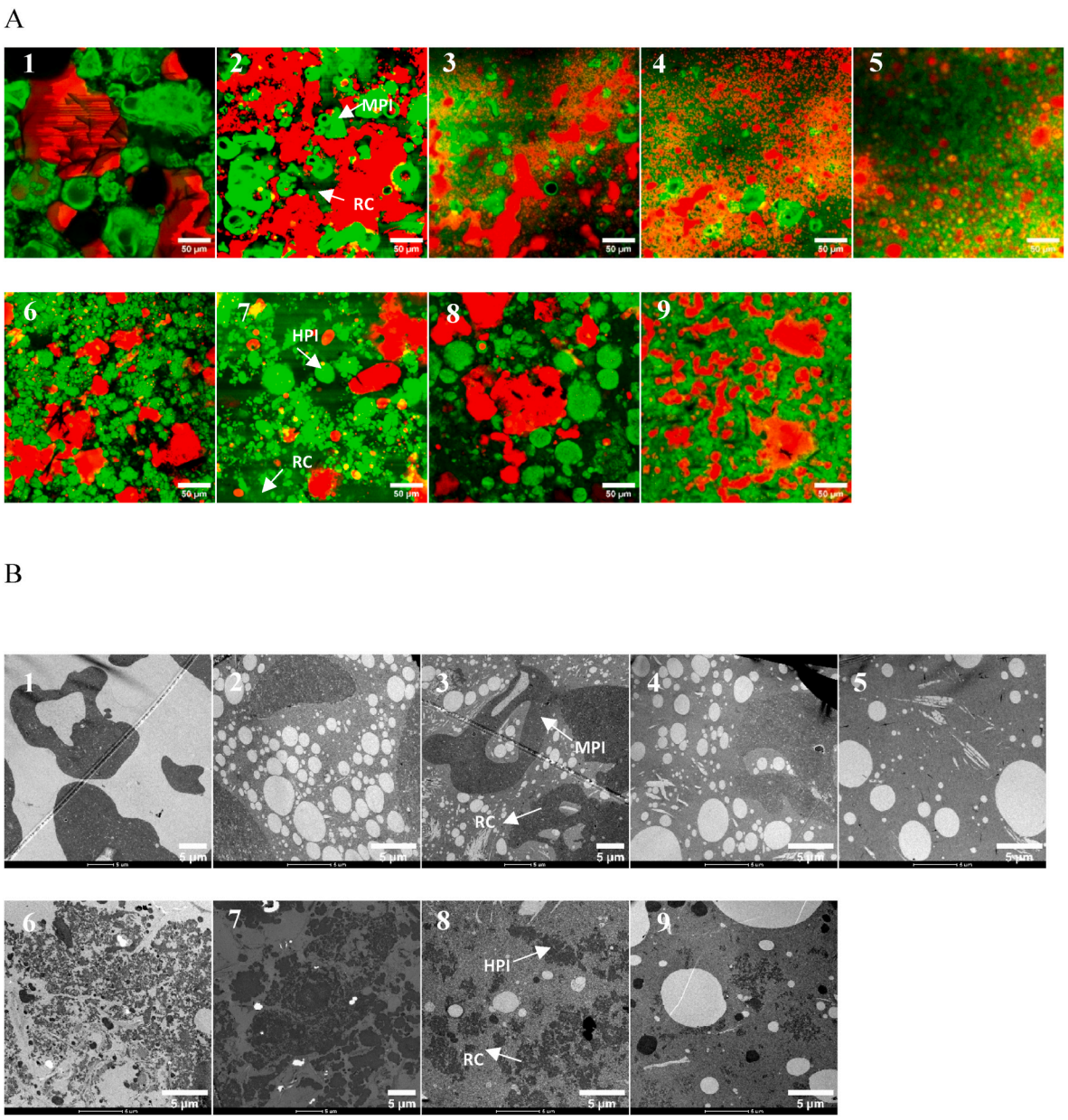

Fig. 3. Representative CLSM (A) and TEM (B) images of mung bean protein (MPI) and hemp protein-based (HPI) hybrid processed cheese analogues. Fat in red and protein in green in CLSM. MPI100: 100 % mung bean protein in cheese (1); MPI70: 70 % mung bean protein, 30 % rennet casein (2); MPI50: 50 % mung bean protein, 50 % rennet casein (3); MPI30: 30 % mung bean protein, 70 % rennet casein (4); RC100: 100 % rennet casein (5); HPI100: 100 % hemp protein in cheese (6); HPI70: 70 % hemp protein, 30 % rennet casein (7); HPI50: 50 % hemp protein, 50 % rennet casein (8); HPI30: 30 % hemp protein, 70 % rennet casein (9). CLSM images scale bars = 50 μm and TEM images scale bars = 5 μm.

values were higher in the mung bean protein-based hybrid cheese. This indicates that a stronger casein-casein network was formed in the mung bean protein system. In other words, hemp protein disrupted the casein-casein interactions more significantly than mung bean protein. Interestingly, G' values of HPI70 and HPI50 exhibited different behaviour than other cheese samples (Fig. 2D). These samples indicate a distinct decrease in G′ and G'' (data not shown) from 20 °C to ~40 °C, followed by an increase in both moduli up to ~60 °C, suggesting network restructuring or protein-protein interactions, and the formation of a more structured yet flexible network. After 60 °C, the moduli plateaued, indicating the formation of a stable structure. However, in the case of HPI30, the low concentration of hemp protein limits its ability to interact with casein. As a result, casein had a more dominant influence, contributing to the gradual decrease in G′ with increasing temperature, without the same network re-structuring observed at high hemp protein concentrations. The hypothesis suggests that the presence of disulphide bonds in hemp protein, rather than in mung bean protein, may facilitate interactions with casein as the temperature increases. This is supported by evidence that heating above a critical unfolding temperature enhances the accessibility of buried thiol (-SH) groups, thereby promoting the formation of intermolecular disulphide bonds (Dapčević-Hadnađev et al., 2018). These results aligned with SDS-PAGE results of a possible interaction between HPI with α_{s2}-casein.

3.3. Microstructure

CLSM analysis was applied to understand protein and lipid distributions within the microstructure of HPCAs (Fig. 3A). In general, the addition of plant proteins to the cheese formulation led to a heterogeneous microstructure, wherein the proteins formed aggregates with a

Table 2
Textural profile of processed hybrid cheese analogues.

	MPI100	MPI70	MPI50	MPI30	HPI100	HPI70	HPI50	HPI30	RC100
Hardness	$806.68^{ab} \pm 53.87$	$649.72^{b} \pm 51.49$	$396.98^{c} \pm 21.62$	$371.69^{c} \pm 30.90$	$297.71^{c} \pm 27.7$	$89.64^{d} \pm 9.02$	n/a	n/a	$821.79^{a} \pm 22.00$
Springiness	$0.38^{a} \pm 0.04$	$0.27^{a} \pm 0.12$	$0.28^{a} \pm 0.02$	$0.30^{a} \pm 0.03$	$0.28^{a} \pm 0.02$	$0.35^{a} \pm 0.05$	n/a	n/a	$0.65^{b} \pm 0.03$
Cohesiveness	$0.05^{a} \pm 0.01$	$0.32^{b} \pm 0.05$	$0.63^{c} \pm 0.03$	$0.75^{c} \pm 0.02$	$0.53^{bc} \pm 0.10$	$0.73^{c} \pm 0.02$	n/a	n/a	$0.69^{c} \pm 0.01$
Chewiness	$14.38^{a} \pm 3.45$	$54.92^{ab} \pm 10.33$	$68.79^{b} \pm 5.21$	$83.91^{b} \pm 14.50$	$41.67^{a} \pm 6.30$	$23.46^{a} \pm 4.93$	n/a	n/a	$370.58^{c} \pm 10.60$
Resilience	0.03^{a}	$0.09^{ac} \pm 0.02$	$0.22^{b} \pm 0.01$	$0.27^{b} \pm 0.01$	$0.18^{bc} \pm 0.05$	$0.19^{bc} \pm 0.02$	n/a	n/a	0.27^{b}

Values within a row not sharing a common superscript differ significantly ($p < 0.05$). Ratios: MPI/HPI100 (100 % plant protein), MPI/HPI70 (70 % plant protein, 30 % rennet casein), MPI/HPI50 (50 % plant protein, 50 % rennet casein), MPI/HPI30 (30 % plant prtein, 70 % rennet casein), RC100 (100 % rennet casein).

non-continuous network (e.g., MPI100, HPI100) with large pools of fat separated from the protein, suggesting that plant proteins may contribute to weaker fat-protein interactions compared to casein. The microstructure differed from the commercial starch-dominated plant-based cheeses observed by Grasso et al. (2021), wherein the distribution of fat globules had a generally spherical shape, stabilised by other hydrocolloids. Similarly, the addition of plant protein to starch-based cheese presented protein aggregates/clusters that were non-homogeneously distributed within the cheese network. With the increasing ratio of RC in the cheese matrix, more fat pools broke down into spherical fat droplets and were trapped in the casein network, resulting in a more continuous cheese network, in agreement with the observation of commercially processed cheeses (Grasso et al., 2021; Ramel & Marangoni, 2017).

Mung bean protein tended to form large, deflated sphere particles ranging from 10 to 100 μm, resulting in a coarse, rough, and granular structure (Fig. 3A (1)). When combined with casein, mung bean protein disrupted the formation of the casein network, especially at high protein levels (e.g. Fig. 3A (2)). This disruption resulted in a non-continuous casein structure and a cheese matrix predominantly composed of mung bean protein. Consequently, fragmented sections of the casein network filled the gaps where the mung bean protein was not interconnected. When HPCAs comprised >50 % RC, the cheese network shifted from being dominated by mung bean protein to casein. Casein prevented the mung bean protein particles from clustering, with mung bean protein particles acting as a filler.

Hemp protein tended to form smaller, denser, and more evenly distributed particles ranging from 1 to 50 μm (Fig. 3A (6)). Similar to mung bean protein, HPCAs at high levels of hemp protein, the cheese matrix primarily comprised hemp protein (e.g. Fig. 3A (7)). A more continuous and smooth casein network was formed with 70 % RC in HPCAs (Fig. 3A (9)). Notably, hemp protein disrupted the casein network more than mung bean protein owing to more hemp protein particles being dispersed in the cheese matrix.

TEM was also applied to provide high-resolution imaging for observing cheese microstructure (Fig. 3B). The micrograph of MPI100 demonstrated a large circular structure (around 30 μm), which is also seen by CLSM (Fig. 3B (1)). The particles were present as individual particles and merged into larger agglomerates (Loveday & Halim, 2024). After adding RC, a distinct boundary was observed between MPI (darker grey) and RC (lighter grey), indicating little or no interaction with casein. In addition, numerous fat droplets with a more homogenous distribution were observed in the casein network rather than in MPI100. Moreover, casein and fat droplets were observed in the hollow part of the MPI aggregation (e.g. MPI30).

TEM micrograph of HPI100 appeared to have a more fragmented and heterogeneous structure. As RC increased, this non-protein inclusion became less noticeable. In addition, TEM confirmed that hemp protein aggregates appeared as small irregular flakes and smaller in size than mung bean aggregates and were dispersed in the cheese matrices. In the mixed system, they were darker in colour than RC (e.g. Fig. 3B (4) and (8)). In fact, the protein aggregation size and shape formed are closely related to the production process, and commercial plant protein isolates often form particulate structures with large protein aggregation and partial or extensive denaturation before heat treatment (Beghdadi et al., 2022; Hadnađev et al., 2018; Loveday & Halim, 2024; Lyu et al., 2023).

3.4. Texture profile of HPCAs

Texture parameters of the HPCAs were examined using a texture analyser (Table 2). Cheese samples of MPI100, MPI70 and RC100 exhibited higher hardness than the other samples. Hardness decreased as the mung bean protein concentration decreased, likely because the network was disrupted by the presence of different protein types in the cheese matrix. Although the total protein content remained at 18 %, the dual-protein system formed independent networks, reducing the effective protein concentration and overall structural strength. In contrast, RC100 formed a smooth and strong network without interference from plant proteins, resulting in higher hardness. In addition, cheese with hemp protein had lower hardness than those with mung bean protein (i.e. HPI100 *vs* MPI100), suggesting a denser network with stronger interactions in the mung bean protein, as observed at the microstructure level. By contrast, hemp protein forms smaller, more uniformly dispersed aggregates, creating a more flexible structure and resulting in lower hardness. As the hemp protein concentration increased, the hardness further decreased accordingly. Moreover, HPI50 and HPI30 were too soft to be tested, therefore, there were no results for these samples.

In addition, springiness indicates how well a cheese sample springs back after deforming during the first compression. It was found that only the RC100 samples showed the highest springiness and chewiness, whereas samples containing plant proteins significantly affected their springiness and chewiness. Cohesiveness is the strength of the internal bonds that make up the cheese structure and how well the cheese can be deformed before it breaks (Rosenthal & Thompson, 2021). Resilience indicates how well a cheese sample resists regaining its original height. With an increasing ratio of casein in the cheese samples, cohesiveness and resilience increased. Moreover, the addition of over 50 % RC to the hybrid cheeses showed similar resilience to RC100. HPI100 cheese showed higher cohesiveness and resilience than MPI100, likely owing to the more uniform distribution of hemp protein in the cheese matrix, allowing for better recovery after deformation. By contrast, mung bean protein forms large aggregates, leading to a denser and more rigid structure in the cheese (Tojan, 2021). This denser structure typically increases the hardness because the larger aggregates create a more compact and less flexible network. However, this rigidity can also reduce resilience because the cheese is less likely to bounce back after being compressed or deformed.

These findings are consistent with those of previous studies (Khiabanian et al., 2022; Mazinani et al., 2020; Omrani Khiabanian et al., 2020) that evaluated the textural properties of feta cheese manufactured from MPC with the addition of plant proteins. The findings indicate that cheese hardness, cohesiveness, springiness, and chewiness decreased with increasing levels of pea or soy proteins. For instance, H. Li, Yang, Chen, et al. (2018) stated that the addition of soymilk hindered the aggregation of skim milk, decreasing gel strength. A similar observation was reported by Monga et al. (2022), in that the presence of globular proteins decreases the compactness of protein structure, which

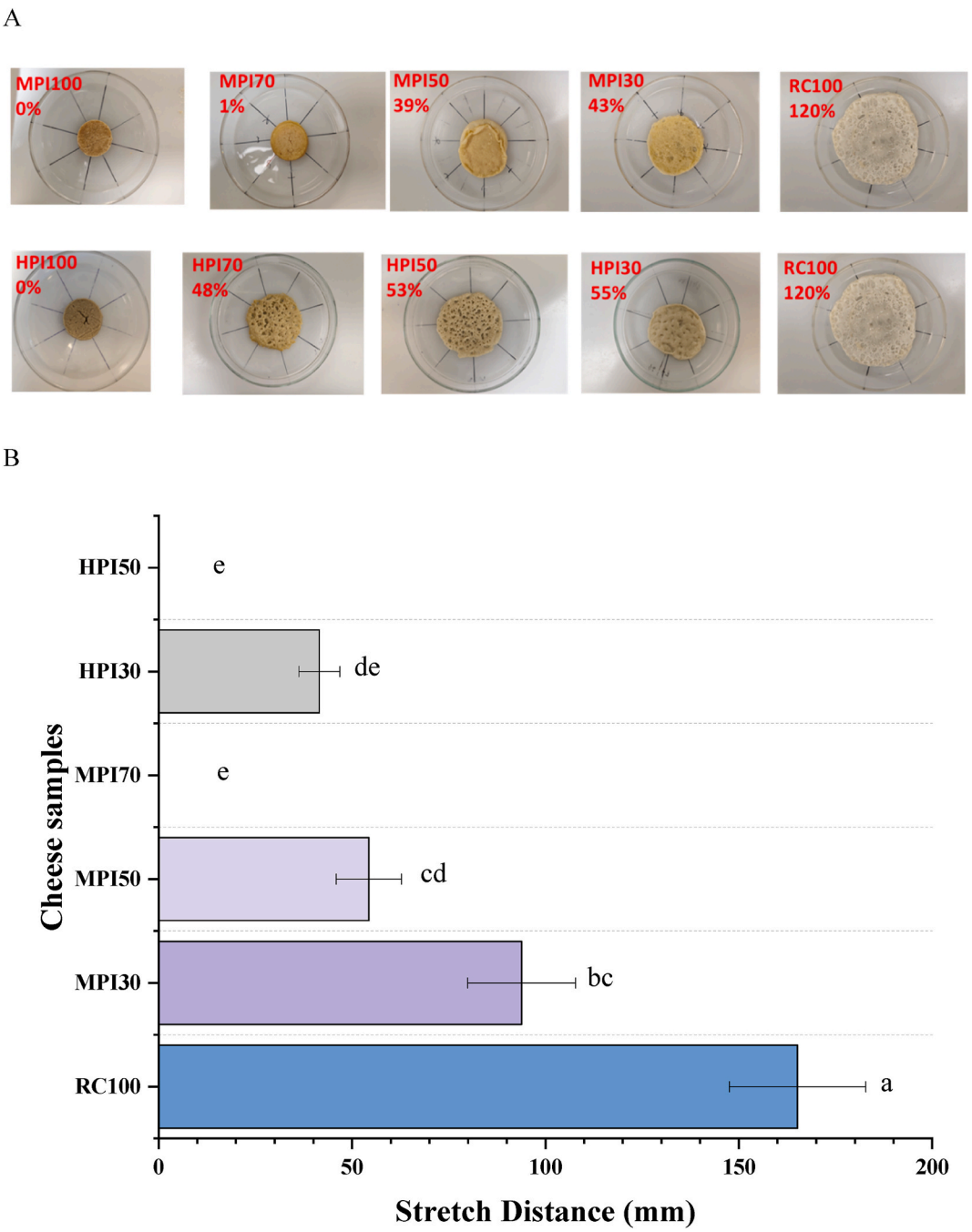

Fig. 4. Representative images (A) of hybrid processed cheese analogues (HPCAs) made with mung bean protein (MPI) or hemp protein (HPI) and rennet casein at varying ratios, after heating at 170 °C for 10 min, with melting index. Stretch distance of hybrid cheeses (B). Values within a row not having common superscripts differ significantly ($p < 0.05$). Ratios: MPI/HPI100 (100 % plant protein), MPI/HPI70 (70 % plant protein, 30 % rennet casein), MPI/HPI50 (50 % plant protein, 50 % rennet casein), MPI/HPI30 (30 % plant protein, 70 % rennet casein), RC100 (100 % rennet).

manifested as a decrease in cohesiveness of hybrid cheese than dairy cheese. Briefly, although hybrid cheeses with plant proteins typically have inferior texture to milk-based cheeses, varying plant proteins and ratios can help match milk protein textures.

3.5. Meltability and stretchability

Meltability is a crucial functional characteristic of processed cheese, defined as its ability to flow and spread when heated, resulting in the visual loss of individual cheese shreds (Guinee, 2011). This property is mainly influenced by the strength of casein–casein interactions (Park et al., 1984). Upon heating, the cheese network softens as milk fat melts > ~40 °C. Moreover, continued heating causes the casein network to contract owing to increased hydrophobic interactions. This contraction reduces contact between casein molecules, weakening the overall network and leading to further softening or melting of the cheese (Lamichhane et al., 2018; Lucey et al., 2003).

Fig. 4A presents melting properties of the samples. Notably, increasing casein content in the hybrid system increased the expansion area. The presence of casein micelles in RC results in extensive protein–protein and protein–fat globule interactions, forming a fibrous casein network. At high temperatures, there is a more rapid relaxation of casein protein-protein bonds and a change to a more liquid-like character. The addition of plant protein can lead to cross-linking among

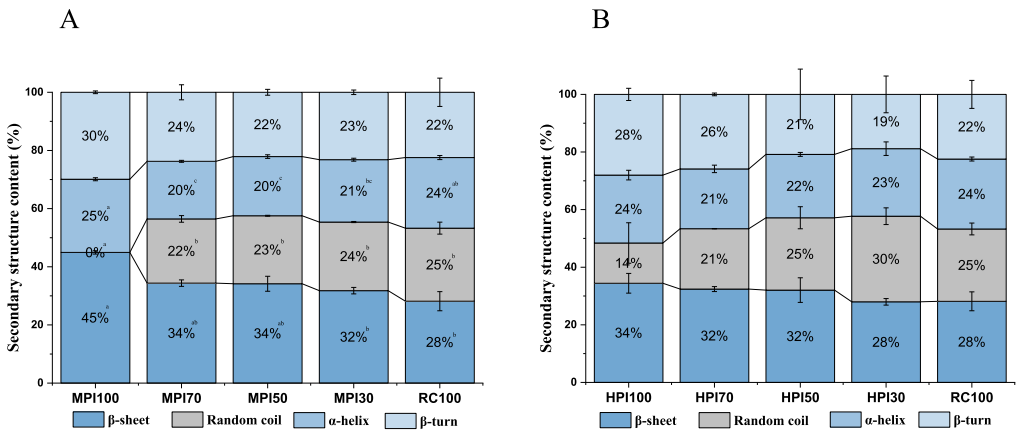

Fig. 5. Secondary structure content of mung bean protein-based hybrid cheeses (A) and hemp protein-based hybrid cheeses (B) by FTIR. Referenced location of secondary structures: β-sheet (1610–1642 cm^{-1}), Random coil (1640–1650 cm^{-1}), α-helix (1650–1660 cm^{-1}) and β-turn (1660–1699 cm^{-1}) (Gawat et al., 2024; Sadat & Joye, 2020). All values are reported as the mean ± SEM, where N = 3 (3 replicates with 3 measurements). Values within a row not having common superscripts differ significantly ($p < 0.05$). Ratios: MPI/HPI100 (100 % plant protein), MPI/HPI70 (70 % plant protein, 30 % rennet casein), MPI/HPI50 (50 % plant protein, 50 % rennet casein), MPI/HPI30 (30 % plant protein, 70 % rennet casein), RC100 (100 % rennet casein).

themselves as well as with caseins at high temperatures, weakening the casein-casein interactions. The pure plant protein-based cheese samples, HPI100 and MPI100, exhibited no melting behaviour, consistent with the previous observations (Grasso et al., 2021), owing to the lack of a continuous protein network.

Hemp protein-based hybrid cheeses (e.g. 48 % in HPI70 and 53 % in HPI50) tend to have higher meltability than those prepared with mung bean protein at the same ratios (e.g. 1 % in MPI70 and 39 % in MPI50). This is more significant at higher plant protein ratios. This may be attributed to the formation of smaller and more uniformly dispersed hemp protein aggregates, as observed in CLSM and TEM micrographs. These structural differences likely disrupted casein-casein interactions more extensively than mung bean protein. Rheological results indicated that this disruption led to weaker casein-casein interactions, facilitating melting. Moreover, the surface of HPI70 and HPI50 exhibited a more porous, honeycombed structure, suggesting that hemp protein in hybrid cheese releases water more effectively, promoting larger expansion during heating. However, as the casein proportion increased in the HPI and MPI hybrid cheese systems, the difference became smaller as casein became dominant.

Stretchability is an important quality attribute of melted cheese. A stretchability test was conducted on the HPCA samples with melting properties from the results mentioned above, excluding MPI100 and HPI100. Owing to the limited sensitivity of the texture analyser, it cannot detect the stretch breaking point of the samples. Thus, the stretch processes were video recorded, and the stretch distance was checked using the texture analyser software and then compared among samples (Fig. 4B). In cheese, stretchability is the ability of the casein network to maintain its integrity without breaking when it is pulled. This depends on intact casein to maintain the strength of the strands with enough calcium and phosphorus (Lucey et al., 2003; Lucey & Fox, 1993). In addition, it is affected by how the casein molecules stick together and handle energy. The stretch test requires casein molecules to be close yet flexible enough to quickly change shape.

In comparison, cheese samples containing only RC exhibited the highest stretchability, characterised by the longest stretch distance. The addition of 30 % or more plant protein in the hybrid system significantly affected the stretchability of HPCAs by interrupting the casein network, changing it from a continuous network to a non-continuous network. Unlike melting properties, hybrid cheeses with mung bean protein exhibited greater stretchability than those with hemp protein at the same ratios (e.g. 93.8 mm in MPI30 *vs* 41.53 mm in HPI30). As discussed in melting behaviour, mung bean protein formed larger aggregates, which interrupt the cheese matrix less frequently but hinder casein flow during melting, thereby reducing meltability but improving stretchability. In other words, the fewer interactions between casein–casein in HPI hybrid cheese samples compared with MPI hybrid cheese samples further decreased stretchability while enhancing meltability. When the cheese is heated, these small hemp protein aggregates in the casein network have less impact on the relaxation of the casein network, allowing it to flow more freely and thereby improving melting properties. However, these small aggregates interrupt the casein network more uniformly, which negatively impacts the cheese stretchability. This results in more points of disruption within the casein network, decreasing stretchability. Another proposed reason may relate to the presence of disulphide bond in hemp protein, which could promote cross-linking with casein at high temperatures, further interrupting the casein network.

3.6. *Analysing protein structure with FTIR*

FTIR spectroscopy measures the vibrational movements of molecules caused by the absorption of infrared radiation by chemical bonds in functional groups. FTIR spectra for HPCAs were recorded in the 450–4000 cm^{-1} range. In protein, the amide I (1600–1700 cm^{-1}) bands are commonly analysed, primarily associated with C=O and N–H stretching, reflecting protein secondary structure depending on hydrogen bonding and conformation of the polypeptide: such as α-helix (1650–1660 cm^{-1}), β-sheet (1610–1642 cm^{-1}), β-turn (1660–1699 cm^{-1}), and random coil (unordered, 1640–1650 cm^{-1}) structures. The amide II band (1480–1580 cm^{-1}), which originates mainly from N–H bending and C–N stretching vibrations, is less commonly used for secondary structure determination due to its lower sensitivity and overlap with other signals (Saji et al., 2024). Thus the amide I bands were analysed and deconvoluted to examine protein structure changes in the hybrid cheese samples (Fig. 5 and Supplementary Fig. S3). MPI and HPI promoted the formation of β-sheet structures, which gradually decreased as the RC content increased (43 % in MPI100, 39 % in HPI100, and 32 % in RC100). This observation is consistent with Sim et al.'s (2021) study, which found that plant proteins tend to have more β-sheet structures, leading to protein aggregation. In particular, MPI had a high β-sheet content, suggesting increased exposure of hydrophobic regions, which may contribute to a firmer and more rigid cheese structure (Jadhav et al., 2024). As RC content increases, more disordered structures were promoted, making the hybrid cheeses more flexible—an important factor for functional properties such as meltability and

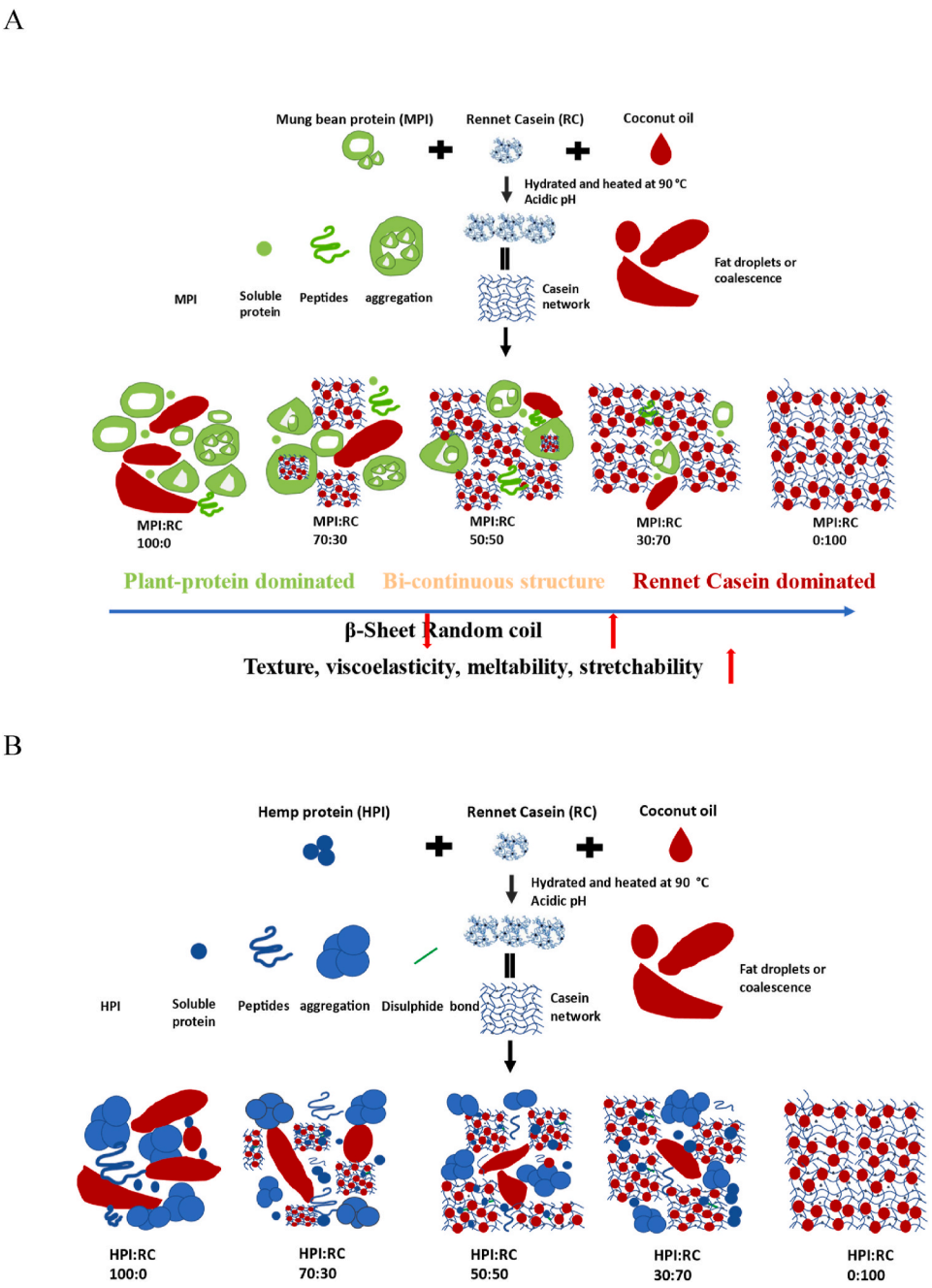

Fig. 6. A schematic diagram summarizing the development of the microstructure of mung bean protein (A) and hemp protein-based hybrid cheeses (B) at different plant protein-to-rennet casein ratios and the relationship between structure and functionality. Ratios: MPI/HPI100 (100 % plant protein), MPI/HPI70 (70 % plant protein, 30 % rennet casein), MPI/HPI50 (50 % plant protein, 50 % rennet casein), MPI/HPI30 (30 % plant protein, 70 % rennet casein), RC100 (100 % rennet casein).

stretchability. MPI100 indicated no random coil structures, whereas HPI100 exhibited a higher proportion, indicating that HPI may provide greater flexibility in cheese structure than MPI. Adding RC to mung bean protein blends (30:70, 50:50, and 70:30) reduced the helical structures in hybrid cheeses. However, the helical structure content did not significantly differ between pure mung bean cheese and pure RC cheese, indicating that the interaction between casein and mung bean protein primarily influences the helical structure in mixed formulations rather than in their pure forms. For hemp protein blends, a similar decreasing trend in the helical structure was observed with the addition of RC, though the changes were not statistically significant. In addition, while the β-turn content showed a reduction in mung bean and hemp protein blends upon the addition of RC, these decreases were not statistically significant. These results suggest that although α-helices and β-turns contribute to the structural properties of the protein networks, they may not be the primary factors influencing the functional characteristics of these hybrid cheeses.

3.7. Structure–functionality relationship proposed in plant protein-casein HPCAs

Fig. 6 presents the development of the microstructure of HPCAs at different plant protein-to-RC ratios and the relationship between structure and functionality. After mixing and heating ingredients, namely, plant protein, RC, coconut oil, emulsifying salts and water, the proteins undergo hydration, interaction with emulsifying salts, denaturation, and

gelation. Particularly, plant proteins exist in various forms after hydration, with a small amount as soluble protein and peptides, but primarily as aggregates. By contrast, casein interacts with itself, solubilizes through emulsifying salts, sequesters calcium ions, and forms a gel-like network. In the absence of casein, the coconut oil does not evenly disperse, forming fat coalescence, whereas, with casein present, coconut oil droplets are evenly dispersed throughout the casein network. At high plant protein ratios, the network is mainly dominated by plant proteins. However, as the proportion of casein increases, a bicontinuous structure develops, wherein plant proteins and casein form independent networks. This transition is accompanied by decreased β-sheet content and increased random coil structures, resulting in a smooth and homogeneous matrix. As casein levels continue to rise, they become the primary structural component, improving viscoelastic and functional properties, whereas plant proteins function as fillers within the matrix. Mung bean protein (Fig. 6A) tends to form larger aggregates than hemp protein (Fig. 6B), which blocks the melting of the casein network during heating. By contrast, hemp protein integrates more into the casein network, leading to greater disruption of its structure. The presence of disulphide bonds in hemp protein may also promote interactions with casein during heating, further contributing to this disruption. This possibly contributes to increased meltability but reduced stretchability compared with mung bean protein.

4. Conclusions

This study provided insights into changes in protein structure and microstructure in hybrid processed cheese (HPCAs) formulated with mung bean protein and RC, as well as hemp protein and RC. Incorporating plant protein into cheese affected its microstructural, textural and functional properties because the formation of an independent protein network was observed and one may affect the other in the cheese matrix. Among the tested formulations, mung bean protein–based HPCAs exhibited greater stretchability, rheological and textural attributes than those containing hemp protein at the same ratios, despite exhibiting low meltability. These differences may be attributed to variations in the size of plant protein aggregates. In addition, the presence of disulphide bonds in hemp protein may enhance interactions with casein at rising temperatures. Overall, blending plant proteins with milk proteins to create hybrid cheese analogues offers promising potential for achieving desired textures and functionalities, depending on incorporation ratios and specific plant proteins used. This study contributes to understanding the structure–functionality relationship in hybrid cheeses and their potential applications in the growing plant-based food industry. In future, other techniques such as confocal Raman microscopy will be used to gain deeper structural insights and distinguish between plant and milk proteins in hybrid cheeses. Additionally, amino acid profiling (e.g., via RP-HPLC) and targeted analyses of disulphide bonding and intermolecular forces will be undertaken to provide more direct evidence of the molecular interactions governing cheese functionality.

CRediT authorship contribution statement

Di Lu: Writing – original draft, Methodology, Investigation, Formal analysis, Data curation, Conceptualization. **Debashree Roy:** Writing – review & editing, Supervision. **Alejandra Acevedo-Fani:** Writing – review & editing, Supervision. **Harjinder Singh:** Writing – review & editing, Supervision. **Mark Waterland:** Writing – review & editing, Methodology. **Aiqian Ye:** Writing – review & editing, Supervision, Resources, Project administration, Funding acquisition, Conceptualization.

Funding

This research work was supported by the Riddet Institute Centre of Research Excellence (CoRE), funded by the New Zealand Tertiary Education Commission.

Declaration of competing interest

The authors declare that they have no known competing financial interests or personal relationships that could have appeared to influence the work reported in this paper.

Acknowledgments

The authors thank the Manawatu Microscopy and Imaging Centre, Massey University, Palmerston North, New Zealand, for supporting the microscopy studies.

Appendix A. Supplementary data

Supplementary data to this article can be found online at https://doi.org/10.1016/j.foodhyd.2025.111688.

Data availability

Data will be made available on request.

References

Auty, M. A. E., Twomey, M., Guinee, T. P., & Mulvihill, D. M. (2001). Development and application of confocal scanning laser microscopy methods for studying the distribution of fat and protein in selected dairy products. *Journal of Dairy Research, 68*(3), 417–427. https://doi.org/10.1017/S0022029901004873

Beghdadi, A., Picart-Palmade, L., Cunault, C., Marchesseau, S., & Chevalier-Lucia, D. (2022). Impact of two thermal processing routes on protein interactions and acid gelation properties of casein micelle-pea protein mixture compared to casein micelle-whey protein one. *Food Research International, 155*, Article 111060. https://doi.org/10.1016/j.foodres.2022.111060

Beliciu, C. M., & Moraru, C. I. (2011). The effect of protein concentration and heat treatment temperature on micellar casein–soy protein mixtures. *Food Hydrocolloids, 25*(6), 1448–1460. https://doi.org/10.1016/j.foodhyd.2011.01.011

Bryant, C. M., & McClements, D. J. (1998). Molecular basis of protein functionality with special consideration of cold-set gels derived from heat-denatured whey. *Trends in Food Science & Technology, 9*(4), 143–151. https://doi.org/10.1016/S0924-2244(98)00031-4

Chen, H., Xu, B., Wang, Y., Li, W., He, D., Zhang, Y., Zhang, X., & Xing, X. (2023). Emerging natural hemp seed proteins and their functions for nutraceutical applications. *Food Science and Human Wellness, 12*(4), 929–941. https://doi.org/10.1016/j.fshw.2022.10.016 [Review].

Dapčević-Hadnađev, T., Hadnađev, M., Lazaridou, A., Moschakis, T., & Biliaderis, C. G. (2018). Hempseed meal protein isolates prepared by different isolation techniques. Part II. Gelation properties at different ionic strengths. *Food Hydrocolloids, 81*, 481–489. https://doi.org/10.1016/j.foodhyd.2018.03.022

Do, D. T., Ye, A., Singh, H., & Acevedo-Fani, A. (2024). Protein bodies from hemp seeds: Isolation, microstructure and physicochemical characterisation. *Food Hydrocolloids, 149*, Article 109597. https://doi.org/10.1016/j.foodhyd.2023.109597

Dobson, S., & Marangoni, A. G. (2023). Methodology and development of a high-protein plant-based cheese alternative. *Current Research in Food Science, 7*, Article 100632. https://doi.org/10.1016/j.crfs.2023.100632

Farahmandfar, R., Tehrani, M. M., Razavi, S. M. A., & Najafi, M. B. H. (2011). Effect of trisodium citrate concentration and soy cheese on meltability of pizza cheese. *International Journal of Food Properties, 14*(4), 697–707. https://doi.org/10.1080/10942910903367621

Fox, P. F., Guinee, T. P., Cogan, T. M., & McSweeney, P. L. H. (2017a). *Cheese structure, rheology and texture*. Springer. https://doi.org/10.1007/978-1-4899-7681-9

Gallier, S., Gordon, K. C., & Singh, H. (2012). Chemical and structural characterisation of almond oil bodies and bovine milk fat globules. *Food Chemistry, 132*(4), 1996–2006. https://doi.org/10.1016/j.foodchem.2011.12.038

Garcia-Fontanals, L., Llorente, R., Valderrama, J., Bravo, S., & Talens, C. (2023). Hybrid spreadable cheese analogues with faba bean and mealworm (Tenebrio molitor) flours: Optimisation using desirability-based mixture design. *Foods, 12*(7), 1522. https://www.mdpi.com/2304-8158/12/7/1522.

Gawat, M., Boland, M., Chen, J., Singh, J., & Kaur, L. (2024). Effects of microwave processing in comparison to sous vide cooking on meat quality, protein structural changes, and in vitro digestibility. *Food Chemistry, 434*, Article 137442. https://doi.org/10.1016/j.foodchem.2023.137442

Grasso, N., Bot, F., Roos, Y. H., Crowley, S. V., Arendt, E. K., & O'Mahony, J. A. (2022). The influence of protein concentration on key quality attributes of chickpea-based alternatives to cheese. *Current Research in Food Science*. https://doi.org/10.1016/j.crfs.2022.09.028

Grasso, N., Roos, Y. H., Crowley, S. V., Arendt, E. K., & O'Mahony, J. A. (2021). Composition and physicochemical properties of commercial plant-based block-style products as alternatives to cheese. *Future Foods, 4*, Article 100048. https://doi.org/10.1016/j.fufo.2021.100048

Grossmann, L., & McClements, D. J. (2021). The science of plant-based foods: Approaches to create nutritious and sustainable plant-based cheese analogs. *Trends in Food Science & Technology, 118*, 207–229. https://doi.org/10.1016/j.tifs.2021.10.004

Guinee, T. P. (2011). Cheese rheology. In J. W. Fuquay (Ed.), *Encyclopedia of dairy sciences* (2nd ed., pp. 685–697). Academic Press. https://doi.org/10.1016/B978-0-12-374407-4.00082-0.

Hadnađev, M., Dapčević-Hadnađev, T., Lazaridou, A., Moschakis, T., Michaelidou, A. M., Popović, S., & Biliaderis, C. G. (2018). Hempseed meal protein isolates prepared by different isolation techniques. Part I. Physicochemical properties. *Food Hydrocolloids, 79*, 526–533. https://doi.org/10.1016/j.foodhyd.2017.12.015

Hu, Y., Cheng, L., Lee, S. J., & Yang, Z. (2023). Formation and characterisation of concentrated emulsion gels stabilised by faba bean protein isolate and its applications for 3D food printing. *Colloids and Surfaces A: Physicochemical and Engineering Aspects, 671*, Article 131622. https://doi.org/10.1016/j.colsurfa.2023.131622

Itoh, T., Garcia, R. N., Adachi, M., Maruyama, Y., Tecson-Mendoza, E. M., Mikami, B., & Utsumi, S. (2006). Structure of 8Sα globulin, the major seed storage protein of mung bean. *Acta Crystallographica Section D, 62*(7), 824–832. https://doi.org/10.1107/S090744490601804X

Jadhav, H. B., Das, M., Das, A., V, G., Choudhary, P., Annapure, U., & Alaskar, K. (2024). Enhancing the functionality of plant-based proteins with the application of ultrasound–A review. *Measurement: Food, 13*, Article 100139. https://doi.org/10.1016/j.meafoo.2024.100139

Khiabanian, N. O., Motamedzadegan, A., Raisi, S. N., & Alimi, M. (2022). Structure–rheology characterization of whey-less feta cheese containing milk protein concentrate/soy protein isolate. *Korea-Australia Rheology Journal, 34*(1), 35–49. https://doi.org/10.1007/s13367-022-00020-3

Kosikowski, F. V. (Ed.). (1977). *Cheese and fermented milk foods* (pp. 337–340). Ann Arbor, MI: Edward Brothers, Inc.

Kovačević, J., Bechtold, T., & Pham, T. (2024). Plant-based proteins and their modification and processing for vegan cheese production. *Macromolecules (Washington, DC, United States), 4*(1), 23–41. https://www.mdpi.com/2673-6209/4/1/2.

Lamichhane, P., Kelly, A. L., & Sheehan, J. J. (2018). Symposium review: Structure-function relationships in cheese. *Journal of Dairy Science, 101*(3), 2692–2709. https://doi.org/10.3168/jds.2017-13386

Li, S., Feng, X., Hao, X., Zhu, Y., Zou, L., Chen, X., & Yao, Y. (2023). A comprehensive review of mung bean proteins: Extraction, characterization, biological potential, techno-functional properties, modifications, and applications. *Comprehensive Reviews in Food Science and Food Safety*. https://doi.org/10.1111/1541-4337.13183. *n/a*(n/a).

Li, H., Yang, C., Chen, C., Ren, F., Li, Y., Mu, Z., & Wang, P. (2018). The use of trisodium citrate to improve the textural properties of acid-induced, transglutaminase-treated micellar casein gels. *Molecules, 23*(7), 1632. https://www.mdpi.com/1420-3049/23/7/1632.

Li, K., Yang, J., Tong, Q., Zhang, W., & Wang, F. (2018). Effect of enzyme modified soymilk on rennet induced gelation of skim milk. *Molecules, 23*(12), 3084. https://doi.org/10.3390/molecules23123084 [Article].

Li, S., Ye, A., & Singh, H. (2021). Physicochemical changes and age gelation in stored UHT milk: Seasonal variations. *International Dairy Journal, 118*, Article 105028. https://doi.org/10.1016/j.idairyj.2021.105028

Loveday, S. M., & Halim, C. (2024). Protein isolates made in the laboratory versus the factory: A case study with mung bean and chickpea. *Sustainable Food Proteins, 2*(2), 89–98. https://doi.org/10.1002/sfp2.1027

Lu, D., Roy, D., Acevedo-Fani, A., Singh, H., & Ye, A. (2025). Investigation of various plant protein ingredients for processed cheese analogues: Physical properties and microstructure compared with milk proteins. *International Journal of Food Science and Technology, 60*(1). https://doi.org/10.1093/ijfood/vvae018

Lucey, J. A., & Fox, P. F. (1993). Importance of calcium and phosphate in cheese manufacture: A review. *Journal of Dairy Science, 76*(6), 1714–1724. https://doi.org/10.3168/jds.S0022-0302(93)77504-9

Lucey, J. A., Johnson, M. E., & Horne, D. S. (2003). Invited review: Perspectives on the basis of the rheology and texture properties of cheese. *Journal of Dairy Science, 86*(9), 2725–2743. https://doi.org/10.3168/jds.S0022-0302(03)73869-7

Lyu, Z., Sala, G., & Scholten, E. (2023). Melting properties of vegan cheese: Effect of emulsion and protein addition on the thermal behaviour of starch gels. *Food Hydrocolloids, 144*, Article 108917. https://doi.org/10.1016/j.foodhyd.2023.108917 [Article].

Mazinani, S., Motamedzadegan, A., Naghizadeh Raeisi, S., & Alimi, M. (2020). Impact of pea protein isolate in partial substitution of milk protein concentrate on the microstructural, rheological, and sensory properties of bacteriologically acidified feta-type cheese. *Journal of Food Processing and Preservation, 44*(6), Article e14448. https://doi.org/10.1111/jfpp.14448 [Article].

Mazinani, S., Motamedzadegan, A., Nghizadeh Raeisi, S., & Alimi, M. (2021). Characterization of bacteriologically acidified feta cheese using soy protein isolate in different substitution percentages: Rheological, microbiological and sensory properties. *Journal of Food Measurement and Characterization, 15*(6), 5515–5527. https://doi.org/10.1007/s11694-021-00973-z [Article].

McSweeney, P. L. H., Ottogalli, G., & Fox, P. F. (2017). Chapter 31 - Diversity and classification of cheese varieties: An overview. In P. L. H. McSweeney, P. F. Fox, P. D. Cotter, & D. W. Everett (Eds.), *Cheese* (4th ed., pp. 781–808). Academic Press. https://doi.org/10.1016/B978-0-12-417012-4.00031-4.

Mendoza, E. M. T., Adachi, M., Bernardo, A. E. N., & Utsumi, S. (2001). Mungbean [Vigna radiata (L.) Wilczek] Globulins: Purification and Characterization. *Journal of Agricultural and Food Chemistry, 49*(3), 1552–1558. https://doi.org/10.1021/jf001041h

Monga, A., Dev, M. J., & Singhal, R. S. (2022). Cottage cheese from blends of fresh green peas (Pisum sativum L.) and dairy milk (pEaneer): Preparation, characterization, and sensory evaluation. *Lebensmittel-Wissenschaft & Technologie, 160*, Article 113263. https://doi.org/10.1016/j.lwt.2022.113263 [Article].

Moradi, D., Ziarati, P., & Sawicka, B. (2021). Physicochemical and rheological properties of lentil milk/inulin blend—A feta cheese analogue. *Legume Science, 3*(4), e80. https://doi.org/10.1002/leg3.80 [Article].

Noronha, N., Duggan, E., Ziegler, G. R., O'Riordan, E. D., & O'Sullivan, M. (2008). Inclusion of starch in imitation cheese: Its influence on water mobility and cheese functionality. *Food Hydrocolloids, 22*(8), 1612–1621. https://doi.org/10.1016/j.foodhyd.2007.11.007

Noronha, N., Duggan, E., Ziegler, G. R., Stapleton, J. J., O'Riordan, E. D., & O'Sullivan, M. (2008). Comparison of microscopy techniques for the examination of the microstructure of starch-containing imitation cheeses. *Food Research International, 41*(5), 472–479. https://doi.org/10.1016/j.foodres.2008.02.008

Omrani Khiabanian, N., Motamedzadegan, A., Naghizadeh Raisi, S., & Alimi, M. (2020). Chemical, textural, rheological, and sensorial properties of wheyless feta cheese as influenced by replacement of milk protein concentrate with pea protein isolate. *Journal of Texture Studies, 51*(3), 488–500. https://doi.org/10.1111/jtxs.12508 [Article].

Ørskov, K. E., Christensen, L. B., Wiking, L., Hannibal, T., & Hammershøj, M. (2021). Imitation cheese – New insights to relations between microstructure and functionality. *Food Structure, 29*, Article 100206. https://doi.org/10.1016/j.foostr.2021.100206

Park, J., Rosenau, J. R., & Peleg, M. (1984). Comparison of four procedures of cheese meltability evaluation. *Journal of Food Science, 49*(4), 1158–1170. https://doi.org/10.1111/j.1365-2621.1984.tb10417.x

Ramel, P. R., & Marangoni, A. G. (2017). Characterization of the polymorphism of milk fat within processed cheese products. *Food Structure, 12*, 15–25. https://doi.org/10.1016/j.foostr.2017.03.001

Rinaldoni, A. N., Palatnik, D. R., Zaritzky, N., & Campderrós, M. E. (2014). Soft cheese-like product development enriched with soy protein concentrates. *Lebensmittel-Wissenschaft & Technologie, 55*(1), 139–147. https://doi.org/10.1016/j.lwt.2013.09.003 [Article].

Rodrigues, A., Maldonado, R., & Freire, M. (2021). *Effect of partial replacement of milk protein by vegetable proteins on the texture of requeijão* (pp. 133–150). https://doi.org/10.1007/978-3-030-61817-9_7

Rosenthal, A., & Thompson, P. (2021). What is cohesiveness?-A linguistic exploration of the food texture testing literature. *Journal of Texture Studies, 52*, 294–302. https://doi.org/10.1111/jtxs.12586

Sadat, A., & Joye, I. (2020). Peak fitting applied to fourier transform infrared and raman spectroscopic analysis of proteins. https://doi.org/10.3390/app10175918.

Saji, R., Ramani, A., Gandhi, K., Seth, R., & Sharma, R. (2024). Application of FTIR spectroscopy in dairy products: A systematic review. *Food and Humanity, 2*, Article 100239. https://doi.org/10.1016/j.foohum.2024.100239

Salgado, A. M., Ozturk, O. K., Hamaker, B. R., & Campanella, O. H. (2023). Matching textural properties of commercial meat and cheese products using zein as the viscoelastic agent and calcium hydroxide as the textural modifier in plant-based formulations. *Food Hydrocolloids, 137*, Article 108323. https://doi.org/10.1016/j.foodhyd.2022.108323 [Article].

Seleet, F., Kassem, J., Bayomim, H., Abd-Rabou, N. S., & Ahmed, N. (2014). Production of functional spreadable processed cheese analogue supplemented with chickpea. *International Journal of Dairy Science, 9*, 1–14. https://doi.org/10.3923/ijds.2014.1.14

Shrestha, S., van 't Hag, L., Haritos, V., & Dhital, S. (2023). Comparative study on molecular and higher-order structures of legume seed protein isolates: Lentil, mungbean and yellow pea. *Food Chemistry, 411*, Article 135464. https://doi.org/10.1016/j.foodchem.2023.135464

Shrestha, S., van 't Hag, L., Haritos, V. S., & Dhital, S. (2023). Lentil and Mungbean protein isolates: Processing, functional properties, and potential food applications. *Food Hydrocolloids, 135*, Article 108142. https://doi.org/10.1016/j.foodhyd.2022.108142 [Review].

Silva, J. V. C., Cochereau, R., Schmitt, C., Chassenieux, C., & Nicolai, T. (2019a). Heat-induced gelation of mixtures of micellar caseins and plant proteins in aqueous solution. *Food Research International, 116*, 1135–1143. https://doi.org/10.1016/j.foodres.2018.09.058

Sim, S. Y. J., Srv, A., Chiang, J. H., & Henry, C. J. (2021). Plant proteins for future foods: A roadmap. *Foods, 10*(8), 1967. https://www.mdpi.com/2304-8158/10/8/1967.

Tang, C.-H., & Sun, X. (2010). Physicochemical and Structural Properties of 8S and/or 11S Globulins from Mungbean [Vigna radiata (L.) Wilczek] with Various Polypeptide Constituents. *Journal of Agricultural and Food Chemistry, 58*(10), 6395–6402. https://doi.org/10.1021/jf904254f

Tojan, S. (2021). *Hybrid paneer (cottage cheese) : Influence of mung bean protein isolate on the texture, microstructure, and gastro-small intestinal digestion in vitro of paneer : A thesis submitted in partial fulfilment of the requirements for the degree of master of food technology*. Palmerston North, New Zealand: Massey University [Masters, Massey University] http://hdl.handle.net/10179/17297.

Tojan, S., Kaur, L., & Singh, J. (2024). Hybrid paneer: Influence of mung bean protein isolate (Vigna radiata L.) on the texture, microstructure, and in vitro gastro-small intestinal digestion. *Food Chemistry, 434*, Article 137434. https://doi.org/10.1016/j.foodchem.2023.137434

Xu, Y., Li, J., Zhao, J., Wang, W., Griffin, J., Li, Y., Bean, S., Tilley, M., & Wang, D. (2021). Hempseed as a nutritious and healthy human food or animal feed source: A

review. *International Journal of Food Science and Technology, 56*(2), 530–543. https://doi.org/10.1111/ijfs.14755

Ye, A., & Hewitt, S. (2009a). Phase structures impact the rheological properties of rennet-casein-based imitation cheese containing starch. *Food Hydrocolloids, 23*(3), 867–873. https://doi.org/10.1016/j.foodhyd.2008.05.004 [Article].

Ye, A., Hewitt, S., & Taylor, S. (2009b). Characteristics of rennet–casein-based model processed cheese containing maize starch: Rheological properties, meltabilities and microstructures. *Food Hydrocolloids, 23*(4), 1220–1227. https://doi.org/10.1016/j.foodhyd.2008.08.016

Yi-Shen, Z., Shuai, S., & FitzGerald, R. (2018). Mung bean proteins and peptides: Nutritional, functional and bioactive properties. *Food & Nutrition Research, 62*. https://doi.org/10.29219/fnr.v62.1290

Zhang, D., Jiang, K., Luo, H., Zhao, X., Yu, P., & Gan, Y. (2024). Replacing animal proteins with plant proteins: Is this a way to improve quality and functional properties of hybrid cheeses and cheese analogs? *Comprehensive Reviews in Food Science and Food Safety, 23*(1), Article e13262. https://doi.org/10.1111/1541-4337.13262

Zhu, P., Huang, W., Guo, X., & Chen, L. (2021). Strong and elastic pea protein hydrogels formed through pH-shifting method. *Food Hydrocolloids, 117*, Article 106705. https://doi.org/10.1016/j.foodhyd.2021.106705